

since the level scheme is not well known. It seems quite likely though that the In results might apply to Cd¹¹¹ as well. To summarize the situation, it appears that the observed yield of the $(\alpha, \alpha\gamma)$ reaction below about 25 Mev can be accounted for by contributions from both evaporation and Coulomb excitation mechanisms. Above 25 Mev the main contribution to the observed yield appears to come from a nuclear direct-interaction mechanism.

The ratio of the total Coulomb excitation and reaction cross sections for In¹¹⁵ is given by the dashed line in Fig. 5. The total reaction cross section was obtained by use of the continuum theory²⁵ with a value of 1.5×10^{-13} cm for the nuclear radius parameter. The two cross sections are about equal at 10 Mev and the ratio decreases sharply with increasing energy so that at the energy corresponding to the Coulomb barrier (15.5 Mev) the ratio is only 0.06. This sharp decrease is due to the much steeper increase with energy of the total reaction cross section for energies below the Coulomb barrier. At higher energies the ratio decreases less sharply as the reaction cross section approaches its asymptotic value. While the contribution of the Coulomb excitation process thus is fairly substantial, it should be kept in mind that this process only affects the $(\alpha, \alpha\gamma)$ reaction to any appreciable extent.

The calculation of the Coulomb excitation cross

section has also been carried out for proton and deuteron bombardment of In¹¹⁵. The calculated excitation function for the In¹¹⁵($d, d\gamma$)In^{115m} reaction is given by the dashed line in Fig. 3. It is seen that the calculated values are lower than the experimental points by at least a factor of 30. This is not surprising in view of the fact that most of the observed yield is probably due to the (d, pn) reaction. The calculated excitation function for the In¹¹⁵($p, p\gamma$)In^{115m} reaction is given by the dashed line in Fig. 4. It is seen that the contribution of the Coulomb excitation process is substantial at the lowest bombarding energy. The calculated cross section at 10 Mev is, on the other hand, much smaller than the experimental value.

ACKNOWLEDGMENTS

The continued interest in this work of Dr. G. Friedlander is appreciated. The author wishes to thank Professor J. M. Miller and Dr. J. Weneser for valuable discussions. Dr. I. Dostrovsky and Dr. Z. Fraenkel kindly performed the Monte Carlo evaporation calculations. The cooperation of Dr. C. P. Baker and the crew of the 60-inch cyclotron is gratefully acknowledged. The chemical yield analyses were performed by Dr. R. W. Stoenner, Dr. J. K. Rowley, and members of the analytical chemistry group.

Nucleon Transfer Reactions in Grazing Collisions of Heavy Ions*

RICHARD KAUFMANN AND RICHARD WOLFGANG
Department of Chemistry, Yale University, New Haven, Connecticut
 (Received August 30, 1960)

Reactions in which several nucleons are transferred between complex nuclei have been studied by measurement of angular distributions and excitation functions of the recoiling projectile residues. The results show that multinucleon transfer does not proceed either through a compound nucleus or through a mechanism in which the Coulomb barrier is not penetrated (such as the tunneling mechanism for single-nucleon transfer). Instead, the data indicate the existence of a "grazing contact" mechanism. In such a grazing reaction, it appears that a high-energy projectile, though deflected by the Coulomb barrier, still penetrates the region of nuclear binding of the target. It moves along the surface of the target, with the zone of contact between the nuclei being frictionally excited and thus preventing formation of a compound nucleus. The system separates after half a rotation, or less, because the repulsive Coulombic and centrifugal forces exceed the nuclear binding force. Depending on the mode of separation, such grazing contact may result in nucleon transfer, inelastic scattering, or breakup of the projectile. At energies well above the Coulomb barrier, such grazing processes appear to represent an important fraction of the geometric cross section.

I. INTRODUCTION

TWO large classes of heavy-ion nuclear reactions have been identified and studied: compound nucleus interactions and various Coulomb scattering processes occurring outside the normal range of nuclear binding forces. This paper explores a third and intermediate

class of heavy-ion reactions which may be termed grazing processes. At bombarding energies only slightly above the Coulomb barrier, the reactions of heavy ions can be separated into two classes. For relatively large impact parameters, the Coulomb barrier is not penetrated and Rutherford scattering, Coulomb excitation,¹

* Contribution No. 1637 from the Sterling Chemistry Laboratory, Yale University.

¹ D. G. Alkhazov, D. S. Andreyev, A. P. Greenberg, and I. N. Lemberg, *Physica* **22**, 1129 (1956).

nucleon transfer by tunneling,²⁻⁴ and combinations of these such as Coulomb excitation followed by the transfer of nucleons⁵ may result. These interactions may be referred to by the collective term of "barrier processes." At smaller impact parameters the projectile can penetrate the Coulomb barrier, but the kinetic energy will be small at the moment of contact. The nuclear bond which is formed between the projectile and target will then amalgamate the nuclei into a compound system which decays at some subsequent time.

At the higher energies which have recently become available, the situation is no longer as clear cut. For relatively large and small impact parameters respectively, the situation as described for low energies still holds (see Fig. 1). But there is now an intermediate range of impact parameters for which the projectile, though partially deflected by the Coulomb field, comes into approximately tangential contact with the target. It may then move along the surface of the target until it reaches a point at which its forward momentum is sufficient to break the nuclear bond formed between the nuclei (Fig. 1). If this process is completed before fusion to a compound system is possible, a grazing collision results. A necessary condition for such a grazing reaction is then that sometime after contact has been made:

Centrifugal force

$$+ \text{Coulomb force} > \text{nuclear binding force.} \quad (1)$$

In Appendix II these forces have been calculated on the basis of the reduction in surface energy caused by the overlap of two spheres whose centers are separated by a distance determined by the trajectory. The limitations of such calculations will be discussed later. Nevertheless, they do indicate that inequality (1) may

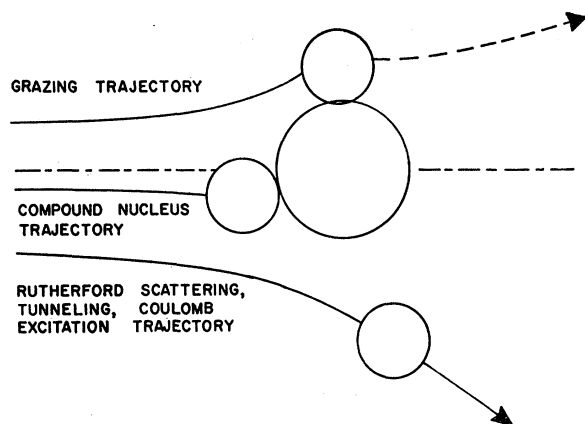


FIG. 1. Typical trajectories representing the three major classes of heavy ion reactions.

² H. L. Reynolds and A. Zucker, *Phys. Rev.* **101**, 166 (1956).

³ J. A. McIntyre, T. L. Watts, and F. C. Jobes, *Phys. Rev.* **119**, 1331 (1960).

⁴ V. V. Volkov, A. S. Pasink, and G. N. Flerov, *J. Exptl. Theoret. Phys. (U.S.S.R.)* **33**, 595 (1957) [translation: *Soviet Phys.-JETP* **6**, 459 (1958)].

⁵ G. Breit and M. E. Ebel, *Phys. Rev.* **104**, 1030 (1956).

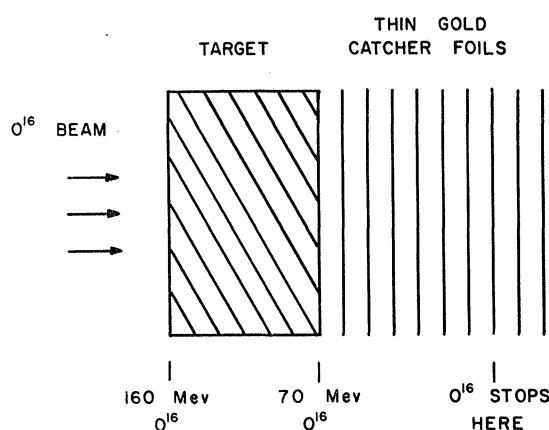


FIG. 2. Experimental apparatus used for the stacked-foil experiments.

be satisfied over an appreciable range of impact parameters at energies above the barrier.

If such grazing reactions occur, they should provide a good mechanism for the transfer of several nucleons. The products of such an interaction would be the residue of the projectile, the residue of the target, and perhaps free nucleons and alpha particles which may be emitted as the system separates. Experimentally, the projectile residues, which should retain a large fraction of their forward momenta, are the easiest to investigate. Such multi-nucleon transfer products have been observed previously,⁶⁻¹⁴ and have been attributed to a variety of reaction mechanisms.

This paper amplifies our earlier communication on multinucleon transfer¹⁰ in which a grazing or "contact transfer" mechanism was proposed.¹⁵ Excitation func-

⁶ K. F. Chackett, J. H. Fremlin, and D. Walker, *Phil. Mag.* **45**, 173 (1954).

⁷ D. G. Alkhazov, Iu. P. Gangrskii, and I. Kh. Lemberg, *J. Exptl. Theoret. Phys. (U.S.S.R.)* **33**, 1160 (1957) [translation: *Soviet Phys.-JETP* **6**, 892 (1958)].

⁸ V. A. Karnaukhov, G. M. Ter-Akopian, and V. I. Khalizev, *J. Exptl. Theoret. Phys. (U.S.S.R.)* **36**, 748 (1959) [translation: *Soviet Phys.-JETP* **9**, 525 (1959)].

⁹ J. J. Pinajian, *Nuclear Phys.* (to be published).

¹⁰ R. Kaufmann and R. Wolfgang, *Phys. Rev. Letters* **3**, 232 (1959).

¹¹ G. A. Chakett, K. F. Chackett, and J. H. Fremlin, *Phil. Mag.* **46**, 1 (1955).

¹² H. L. Reynolds, D. W. Scott, and A. Zucker, *Phys. Rev.* **102**, 237 (1956).

¹³ J. Beydon, R. Chaminade, M. Crut, H. Faraggi, J. Olkowsky, and A. Papineau, *Nuclear Phys.* **2**, 593 (1956/7).

¹⁴ J. H. Fremlin, 1957 Moscow Convention (unpublished).

¹⁵ A somewhat different line of evidence for grazing mechanisms from the transfer reactions used here and in our original paper (reference 10) has recently been reported by Almqvist, Bromley, and Kuehner [E. Almqvist, D. A. Bromley, and J. A. Kuehner, *Phys. Rev. Letters* **4**, 515 (1960)]. Certain resonances in the $C^{12}-C^{12}$ excitation functions are interpreted [E. Vogt and H. McManus, *Phys. Rev. Letters* **4**, 518 (1960); R. H. Davis, *Phys. Rev. Letters* **4**, 521 (1960)] as due to a short-lived "molecular state" formed between projectile and target. In a sense, these "molecular states" represent the lower energy limit of grazing reactions. The present study deals primarily with higher energies, in which the time of the event becomes too short, and the available energy too large to permit discussion of the collision in terms of a well-defined, quasi-equilibrated intermediate complex or molecular state.

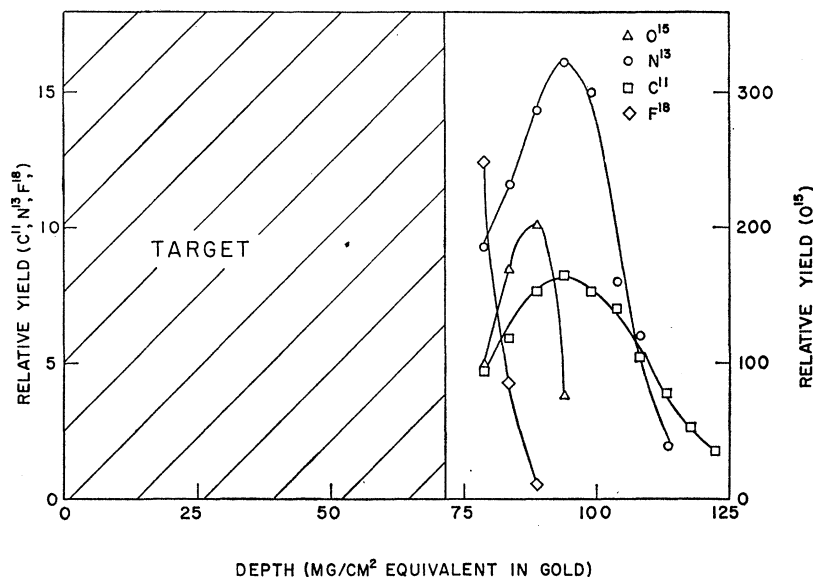


FIG. 3. Results of a typical stacked-foil experiment. Nucleon transfer products produced by a 160-Mev O^{16} beam recoil from the 56 mg/cm² Sn target and come to rest in gold catcher foils.

tions and angular distributions of products expected from grazing transfer reactions are reported. The observations are compared with the predictions of several conceivable mechanisms in order to examine the thesis that they are consistent only with a grazing interaction. (In particular, a mechanism proposed by Zucker¹⁶ as possibly offering an alternative explanation of the data used in our original formulation of the grazing contact mechanism is examined in some detail.) The data are then used to attempt to provide a more detailed model of the postulated grazing process.

II. EXPERIMENTAL METHODS AND RESULTS

A. Stacked Foil Experiments

A preliminary set of experiments was carried out in order to determine if cross sections for multinucleon transfer processes are large enough to permit a detailed study of the interaction, and to determine the approximate energy distribution of the products. The target assembly (Fig. 2) consisted of a target followed by a stack of thin (5–10 mg/cm²) gold catcher foils. The target thickness was adjusted so the beam would pass through the target and so the emerging beam would have an energy well below the Coulomb barrier of gold. Any radioactive products detected in the gold foils were therefore assumed to have recoiled into the catchers from the target material. Details of the experimental method are given in Appendix I. Aluminum, copper, and tin targets were used.

The activities detected in a typical run are plotted in Fig. 3 as a function of depth of recoil into the gold foils. Products lighter than the projectile exhibit a peak in activity at some depth in the catcher foils. These peaks correspond to the retention of about 90% of the

energy per nucleon of the projectile. The peak width arises in large part from the use of thick targets in which interactions can take place at various depths and energies. After correcting for this, it appears that the recoil energy spread of the single-nucleon products is narrow, but that this spread increases as more nucleons are transferred. The lowest energy products detected retain about 75% of the energy per nucleon of the projectile.

Total cross sections averaged over the energy range from about 10 Mev per mass unit to 4 or 5 Mev per mass unit are given in Table I. This energy interval has a different significance for the various targets. Even the lowest energies are appreciably above the Coulomb barrier of aluminum, although they are not much above that of tin. The ratio of yields of two products from a given beam and target are more significant. The ratio of multinucleon to single-nucleon transfer cross sections is seen to be relatively independent of the beam and of the target material used.

B. Angular Distribution Experiments

Angular distributions were measured with the apparatus shown in Fig. 4. A 7.35 mg/cm² rhodium foil was mounted on the center line of the cylindrical target chamber. The beam energy was degraded by about 10 Mev while passing through the target. Catcher foils were taped to the inside of the target chamber so that each catcher foil stopped products which recoiled from the target material in a certain angular interval. Products were detected by observation of the positron annihilation gamma rays. Corrections were made for activity produced by beam particles which were scattered in the target and which then reacted while stopping in the catcher foils. Experimental details are given in Appendix I.

Results are plotted in two forms with angles given

¹⁶ A. Zucker, Phys. Rev. Letters 4, 21 (1960).

TABLE I. Thick-target cross sections (in millibarns) for the production of nucleon transfer products averaged over the energy range of 10 Mev per mass unit to 4 or 5 Mev per mass unit, and ratios of these cross sections.

| Target | Reaction ^a Error Beam | $(-n)$ $\pm 30\%$ | | | $(-p2n)$ $\pm 50\%$ | | $(-2p3n)$ $\pm 50\%$ | $(-p2n)/(-n)$ $\pm 20\%$ | | $(-2p3n)/(-n)$ $\pm 20\%$ |
|--------|--|----------------------|-----------------|-----------------|------------------------|-----------------|-------------------------|-----------------------------|-----------------|------------------------------|
| | | C ¹² | N ¹⁴ | O ¹⁶ | F ¹⁹ | N ¹⁴ | O ¹⁶ | N ¹⁴ | O ¹⁶ | O ¹⁶ |
| Al | 11 | | | 20 | | | 4.0 | | 0.20 | 0.12 |
| Cu | 16 | | 28 | 29 | 51 | ≤ 8 | 4.7 | ≤ 0.29 | 0.16 | 0.10 |
| Sn | 6 | | (20) | 7.9 | | (4.2) | 1.4 | 0.21 | 0.18 | 0.10 |

* To remove indicated number of nucleons from projectile.

in the center-of-mass system (Appendix I). Cross sections differentiated with respect to solid angle ($d\sigma/d\Omega$) are commonly used in nucleon transfer studies, and are shown here in order to compare the present results to those already available on single-nucleon transfer.²⁻⁴ This is not the best way to present results of a grazing interaction since products are preferentially emitted in a plane defined by the incident trajectory of the projectile and the center of the target nucleus. Products which are emitted isotropically with respect to the azimuthal angle (the angle between beam and recoil directions) but are restricted to this plane, will follow a $1/\sin\theta$ curve on a differential cross section ($d\sigma/d\Omega$) plot. This is a result of the relationship between the derivative of the cross section with respect to the azimuthal angle ($d\sigma/d\theta$) and the derivative with the solid angle ($d\sigma/d\Omega$):

$$\frac{d\sigma}{d\theta} = \frac{d\sigma}{d\Omega} \frac{d\Omega}{d\theta}; \quad d\Omega = 2\pi \sin\theta d\theta. \quad (2)$$

Because of the restriction of products to a given plane, deviations from a constant value of $d\sigma/d\theta$ at various angles are more significant than deviations from a constant value of $d\sigma/d\Omega$. It should also be noted that the area under a plot of $d\sigma/d\theta$ vs θ is proportional to the total cross section, so a shift in the average angle of emission becomes evident.

Results of a bombardment of Rh by O¹⁶ are shown plotted in these two forms in Figs. 5 and 6. The most obvious feature is that all multinucleon transfer products exhibit similar angular distributions, tending toward a maximum near zero degrees. By contrast, the single-nucleon transfer product has its most prominent peak near 20°, while the other products show no structure

near this angle. Such a peak has been observed previously in other systems involving single-nucleon transfer²⁻⁴ and is ascribed to a tunneling or virtual-state mechanism. However, at smaller angles the differential cross section ($d\sigma/d\Omega$) of the single-nucleon transfer product appears to increase again, paralleling the increase for multinucleon transfer. This upturn is not far outside the probable error in any given experiment, but is believed to be real since it is observed in all runs. The appearance of the data suggest that a similar mechanism is responsible for the maxima near zero degrees observed for all products.

Differential cross sections ($d\sigma/d\Omega$) of products produced by N¹⁴ and F¹⁹ beams on a Rh target are shown in Figs. 7 and 8. These curves include products resulting from the pickup of an alpha particle (Fig. 7) and the loss of as many as eight nucleons (Fig. 8). Nevertheless, the qualitative appearance of these results is identical to that just described for O¹⁶ bombardments.

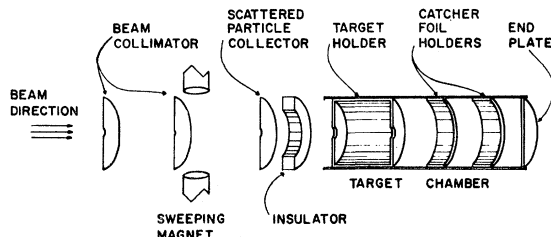


FIG. 4. Experimental apparatus used for the measurement of the angular distributions of nuclear transfer products.

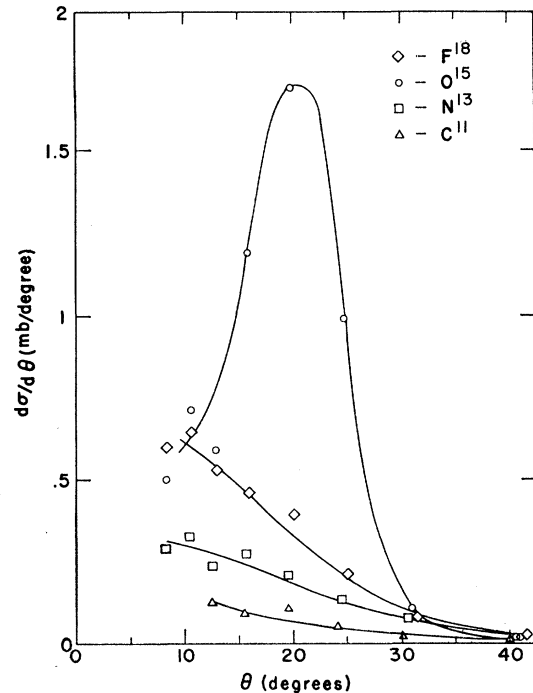


FIG. 5. Differential cross sections with respect to the azimuthal angle are shown for products of the reaction of 160-Mev O¹⁶ with a 7.35 mg/cm² Rh target.

TABLE II. Thin-target cross sections for the production of nucleon transfer products from several beams on a Rh target, for 10 Mev/nucleon lab energy. Listed in each case are the reaction product observed and the cross section σ in millibarns, followed in parentheses by the excitation energy, $-Q$, in Mev which would be required if the projectile were to break up to give the observed product as a result of Coulomb excitation.

| Reaction \ Beam | C ¹² | N ¹⁴ | O ¹⁶ | F ¹⁹ |
|-----------------------|--|----------------------------|----------------------------|----------------------------|
| Loss of projectile | | | | |
| (-n) | C ¹¹ , 15(18.7) | N ¹³ , 20(10.5) | O ¹⁵ , 27(15.6) | F ¹⁸ , 65(10.4) |
| (-p2n) | | C ¹¹ , 5(22.7) | N ¹³ , 7(25.0) | |
| (-2p3n) | | | C ¹¹ , 3(25.9) | |
| (-2p4n) | | | | N ¹³ , 3(24.4) |
| (-3p5n) | | | | C ¹¹ , 2(33.1) |
| Pickup by projectile | | | | |
| (+p) | N ¹³ , 3.2(...) | O ¹⁵ , 6(...) | | |
| (+pn) | | | F ¹⁸ , 15(...) | |
| (+2p2n) | | F ¹⁸ , 1.5(...) | | |
| (+3p3n) | F ¹⁸ , <1(...) | | | |
| Stability of products | | | | |
| | C ¹¹ → Be ⁷ + α | | Q = -7.6 Mev | |
| | N ¹³ → C ¹² + p | | Q = -1.95 Mev | |
| | O ¹⁵ → N ¹⁴ + p | | Q = -7.4 Mev | |
| | F ¹⁸ → N ¹⁴ + α | | Q = -4.4 Mev | |

Cross sections obtained by integrating angular distributions ($d\sigma/d\theta$) extrapolated to zero degrees, are shown in Table II. The multinucleon transfer cross sections do not depend strongly upon the Q of the reaction or upon the stability of the product which is detected.

Reduced energy beams of O¹⁶ were used to obtain excitation functions. The angular distributions from

reduced energy beams are very similar to those from higher energy beams (Fig. 9). Excitation functions for the products detected from the reaction between O¹⁶ and Rh are shown in Fig. 10. The most striking feature here is that the multinucleon transfer cross sections drop off much more rapidly with decreasing energy than the single-nucleon transfer cross sections. This is more clearly evident from the plot of the ratio of single to

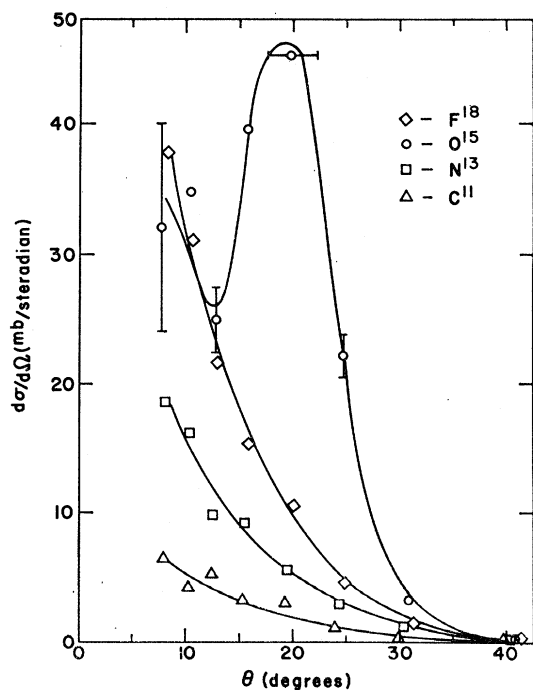


FIG. 6. Differential cross sections with respect to the solid angle are shown for products from the reaction of 160-Mev O¹⁶ with a 7.35 mg/cm² Rh target.

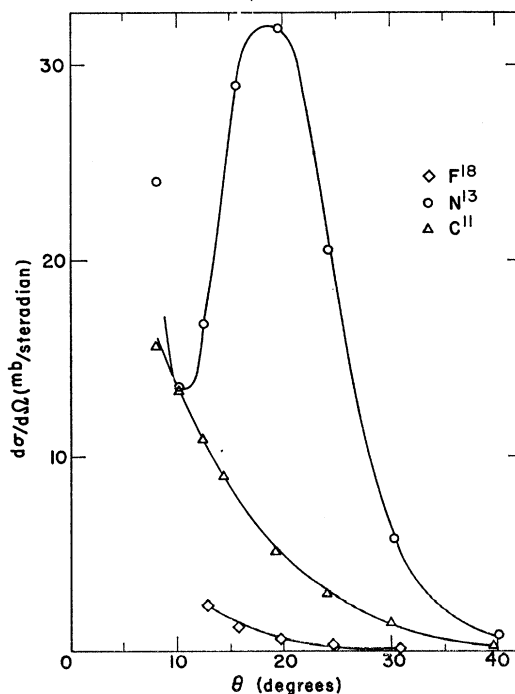


FIG. 7. Differential cross sections with respect to the solid angle are shown for products from the reaction of 140-Mev N¹⁴ with a 7.35 mg/cm² Rh target.

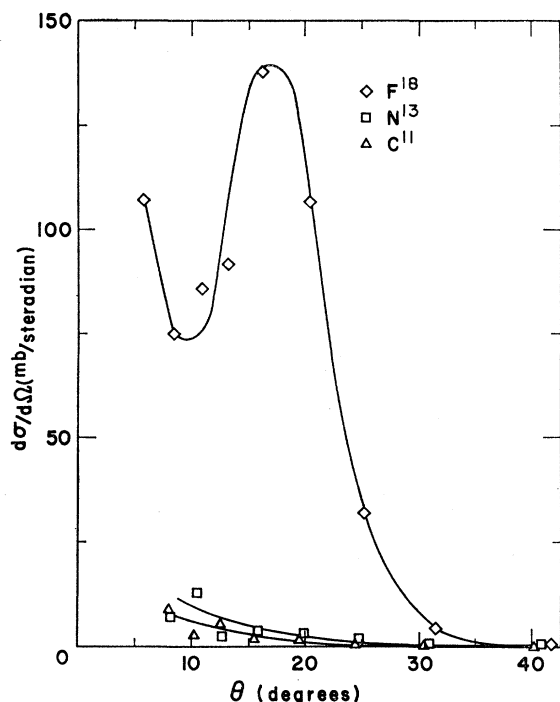


FIG. 8. Differential cross sections with respect to the solid angle are shown for products from the reaction of 190-MeV F^{19} with a 7.35 mg/cm² Rh target.

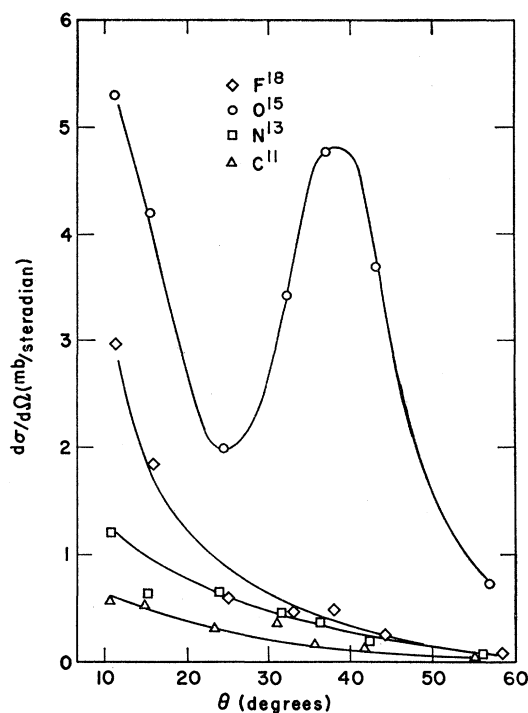


FIG. 9. Differential cross sections with respect to the solid angle are shown for products from the reaction of 101-MeV O^{16} with a 7.35 mg/cm² Rh target.

multinucleon cross sections shown in Fig. 11. Multinucleon transfer products appear to have a threshold at about 80 Mev (Coulomb barrier is 55 Mev).

C. Recoil Range of Products

The recoil range of the products was measured by replacing the single catcher foil at any given angle in the angular distribution apparatus by a stack of thin catchers. These ranges were then converted to recoil energies (Appendix I) and the results are plotted in Fig. 12 as the differential cross section per unit energy interval per degree as a function of energy. This confirms the results of the thick-target experiments, and also gives the energy spread of the deuteron pickup product, (F^{18}). The arrows in Fig. 12 show the energies which C^{11} , N^{13} , and O^{15} would retain if there were no change in velocity due to the interaction, and the arrow labeled O^{16} shows the total beam energy. In all cases, products retain on the average about 90% of the energy expected if there were no change in velocity, and the energy spread increases as more nucleons are transferred.

III. POSSIBLE MECHANISMS FOR MULTI-NUCLEON TRANSFER

Before comparing these results to predictions of a grazing contact model, a number of other possible processes must be considered to see if it is really necessary to postulate a new mechanism. In this section, experi-

mental data will be compared to the predictions of these models.

Compound nucleus processes. A compound nucleus process such as the evaporation of heavy particles or the fission of a compound system may be possible. Any system with a lifetime much greater than the period of a nuclear revolution should distribute products symmetrically about 90°. Figure 13 shows the distribution of nucleon transfer products from the 160-MeV O^{16} bombardment of Rh^{108} in the backward as well as forward directions. It appears that backward recoils are quantitatively negligible compared to those in the forward direction. Identification of products in the backward direction is not certain, so these results give only an upper limit. The evident lack of symmetry about 90° excludes a compound nucleus mechanism as a major contributor to the observed cross sections.¹⁷

Tunneling mechanisms. Mechanisms in which a nucleon tunnels through the Coulomb barrier separating two nuclei have been shown to be important in single-

¹⁷ A peak at 180° in the differential cross sections of the observed products would not necessarily imply that these products were produced by a compound nucleus interaction. Such a distribution could be produced by a grazing contact mechanism in which the system remains bound through a rotation of about 300°. This could be the result of the formation of a semistable osculating system as proposed by Almqvist, Bromley, and Kuehner,¹⁸ by Vogt and McManus,¹⁸ and by Davis¹⁸ in discussing formation of "molecular states" at energies near that of the coulomb barrier.

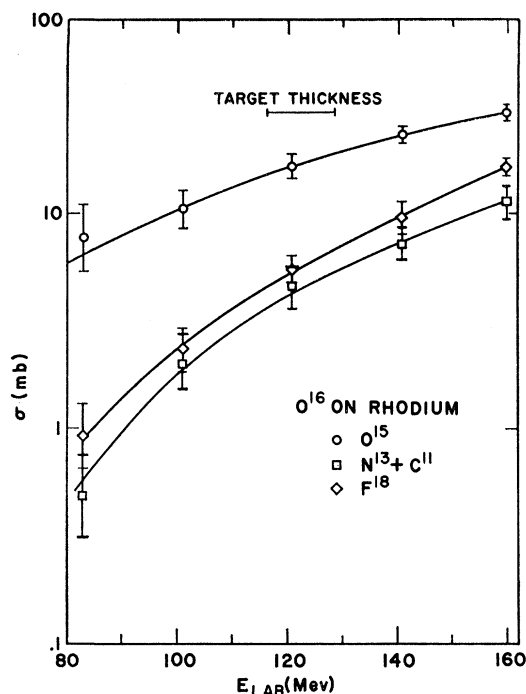


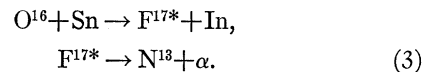
FIG. 10. Excitation functions of nucleon transfer products produced in the O^{16} bombardment of a Rh target.

nucleon transfer.^{2-4,18,19} They predict angular distributions which are peaked at an angle just below the Rutherford scattering cutoff. This is due to the strong dependence of the probability of tunneling upon the distance separating the nuclei. Such angular distributions are observed for single-nucleon transfer products, but multinucleon transfer products show low cross sections with no structure at the angle at which this peak would be expected. If the angular distribution of the multinucleon transfer products were nevertheless interpreted as resulting from a barrier process, such as tunneling, the smaller net deflections would indicate that multinucleon transfer occurs in much more distant collisions than does single-nucleon transfer. If anything, of course, the reverse would be expected. The alternative explanation, that tunneling cross sections are very sharply reduced if more than one nucleon is transferred, is quite reasonable.

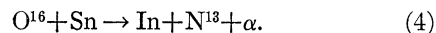
An upper limit can be set for the cross section for transfer of several nucleons by tunneling. For example, F^{18} is detected from the reaction of a N^{14} beam on a Rh target. No evidence of a peak is detected at the angle of the single-neutron transfer peak, and the integrated cross section of F^{18} near this angle is about 0.5 mb. Therefore, it appears that tunneling of an alpha particle to a state with less than 4.4 Mev of excitation energy (the energy required for particle emission from F^{18}) has a cross section of less than 0.5 mb. The cross

section for the transfer of a single neutron from N^{14} to Rh is 20 mb, so alpha-particle tunneling is at least 40 times less probable than neutron transfer in this case.

Zucker,¹⁶ in commenting on some of our preliminary results,¹⁰ has suggested that they could be accounted for by a two-step process involving the transfer of a single nucleon followed by de-excitation of the projectile by particle emission. For example, N^{13} could be produced in the reaction of an O^{16} beam on tin by the following series of reactions:



Zucker also proposed that these processes may occur simultaneously as a three-body disintegration:



In support of this thesis, our results on cross sections and on the greater energy spread of the multinucleon as opposed to single-nucleon transfer products were cited.¹⁶ These results are, however, also consistent with the grazing contact model and do not provide a critical means for choosing between it and Zucker's hypothesis. Two other aspects of our results provide much less ambiguous criteria for making such a choice.

1. According to Zucker's mechanism, the angular distribution of multinucleon transfer products would be expected to follow that for single-nucleon transfer products, though with some spreading of the peak due to the emission of nucleons from the excited single-

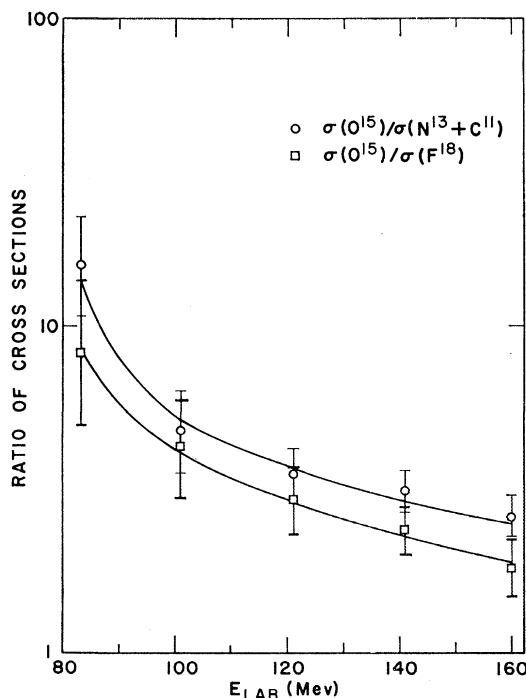


FIG. 11. Ratio of single-nucleon to multinucleon transfer cross sections for the system O^{16} and rhodium.

¹⁸ G. Breit, Phys. Rev. **102**, 549 (1956).

¹⁹ G. Breit and M. E. Ebel, Phys. Rev. **103**, 958 (1956).

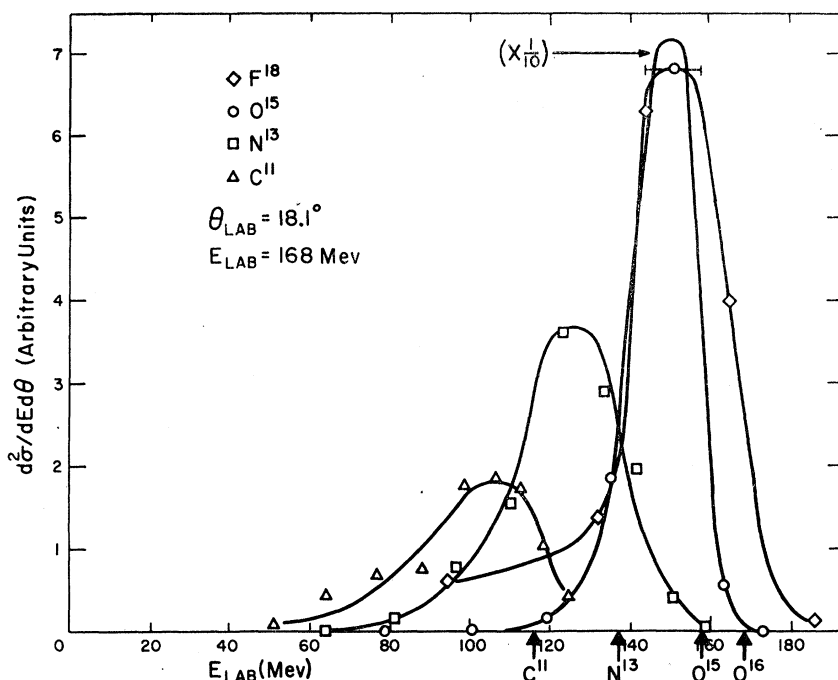


FIG. 12. Differential cross sections with respect to energy and angle for nucleon transfer products as a function of energy. Arrows show energies expected if the velocity of the projectile is not changed during the transfer. The arrow labeled O^{16} shows total beam energy.

nucleon transfer product. Yet the observed angular distributions for single-nucleon and multinucleon transfer are qualitatively quite different. Emission of a 35-Mev alpha by the excited F^{17} [Eq. (3)] at an angle normal to its trajectory would be required to eliminate the peak observed for single-nucleon but not for multinucleon transfer. Even then, the average angle of emission for the two types of products would still be different by 10° . In order to fit the observed angular distribution, emission of high-energy (at least 35-Mev alphas) unobserved particles polarized at about 90° to the beam direction and in the plane of the scattered projectile would be required. It is difficult to conceive of a mechanism by which such particles could be produced. In any case, if they were emitted with the required cross section, they would have been observed in experiments of Knox, Quinton, and Anderson.²⁰

2. Products heavier than the projectile cannot, of course, be produced by the breakup of single-nucleon transfer products and would have to result from another mechanism. It was noted previously that the angular distributions and excitation functions of products formed from the pickup of nucleons by the projectile are very similar to those of products formed from the loss of nucleons from the projectile. This would be a very unlikely coincidence unless similar mechanisms were involved. From this point of view also, the breakup of single-nucleon transfer products fails to account for the observed results.

Coulomb breakup. Mechanisms involving the use of energy from the Coulomb field must be considered as

possibly causing the breakup of projectiles. For instance, O^{16} could be Coulomb excited and then break up to give an alpha particle, a neutron, and C^{11} . To account for the experimental angular distribution, this excitation must take place preferentially at very large distances of closest approach (20–40 f). (Or alternatively, polarized alpha particles and nucleons must be emitted. However, the previous arguments against the production of such polarized particles in the breakup of single-nucleon transfer products also apply to Coulomb breakup.) Since about 25 Mev of excitation energy is required to produce the observed products by Coulomb breakup, it does not seem plausible that these high energies can be provided with high probability (cross sections at least in the tens of millibarns are required) from very distant interactions. Furthermore, if distant interactions were important, a high reaction threshold would not be expected. Finally, this mechanism again fails to account for products heavier than the projectile, and, as previously noted, these seem to be formed by the same type of mechanism that yields products lighter than the projectile.

IV. GRAZING CONTACT MODEL

The considerations in the previous section show that it is unlikely that either compound nucleus mechanisms or the various processes associated with Coulomb scattering can account for the data on multinucleon transfer. It appears that another type of interaction is indeed necessary, and that a grazing contact model is in accord with the experimental observations.

The strongly forward peaked angular distributions of the multinucleon transfer products (Figs. 5–8) are

²⁰ W. J. Knox, A. R. Quinton, and C. E. Anderson, Phys. Rev. Letters **2**, 402 (1959).

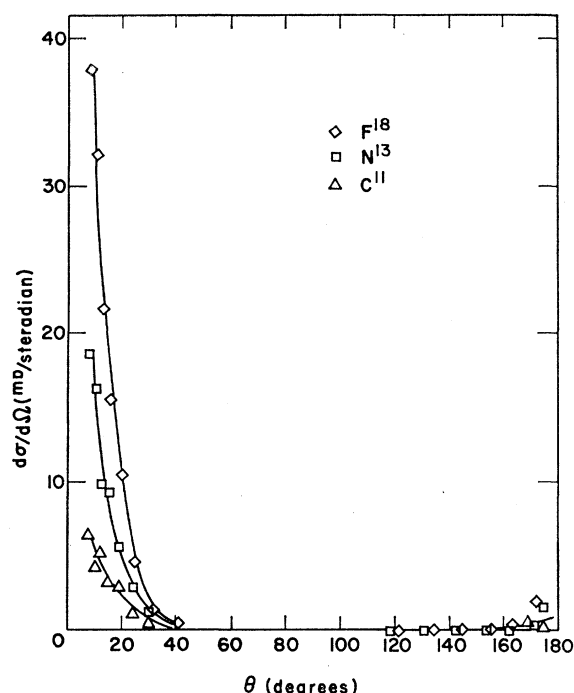


FIG. 13. Differential cross sections of nucleon transfer products from the reaction of 160-Mev O^{16} with Rh in the backward as well as the forward direction. Cross sections in the backward direction are only upper limits since identification of the products is uncertain.

a rather natural result of the penetration of the attractive nuclear potential of the target. This counteracts the repulsion due to the Coulomb field and decreases the net deflection (see Fig. 1). Thus the angular dependence $d\sigma/d\theta$ of the cross sections for 160 Mev O^{16} on Rh (Fig. 5) appears to approach a flat maximum near zero degrees.²¹ An approximate calculation (Appendix II) shows that the formation of a nuclear bond of about 10 Mev between O^{16} and Rh^{108} in grazing collisions will shift the deflection of a 160-Mev projectile from the Rutherford scattering cutoff at 24 degrees to about 10 degrees.

The apparent double maxima in the angular distributions of single-nucleon transfer products (see Figs. 6, 7, 8) indicate the existence of two mechanisms for the formation of these products. One is, of course, the tunneling mechanism²⁻⁴ which has a maximum proba-

bility when the particles approach as closely as possible without penetrating the Coulomb barrier (see Fig. 1). The result is a maximum in the angular distribution near the Rutherford scattering cutoff angle. A closer approach results in penetration of the attractive potential of the target and a grazing collision results. This is clearly distinguishable from tunneling because it results in a smaller net deflection and a second peak in the angular distribution (when plotted as $d\sigma/d\Omega$), which corresponds to the maximum observed for multinucleon transfer products.

It will now be useful to examine the grazing contact model in some detail. In this discussion we use classical mechanics throughout. This is quite well justified since for the systems involved the deBroglie wavelengths ($\lambda = h/mv$) are very small compared to distance of closest approach ($R_{min} = Z_1 Z_2 e^2 / E$). Also, the angular momenta of the colliding systems are large compared to the intrinsic spins of target and projectile.

Consider the incident particle as penetrating the Coulomb barrier at a grazing trajectory. If the initial energy was low, the kinetic energy remaining at this point will be low, and the two drops of nuclear matter will be drawn together by the bond thus formed. However, at higher energies, the projectile will tend to continue tangentially along the surface of the target. This relative motion will cause the volume of contact at the neck of the dumbbell-shaped system to become excited by what is essentially a frictional effect. As the nucleons from this hot region diffuse into the main masses of nuclear matter on each side, the excitation will spread and the motion of the two masses will tend to become rotationally coupled. This process is governed by the rate of diffusion of nucleons which is comparable to the velocity of the nuclei themselves. It is therefore to be expected that well before this coupling is complete, the orbit of the main incident mass will arrive at a point where its remaining excess forward momentum plus the Coulomb repulsion will cause it to separate. Our observation that the mean energy per nucleon of the products is about 90% of that of the incident particle should thus not be unexpected. The breadth of this distribution, with some products having as little as 75% of the incident energy per nucleon, also becomes plausible. (Note by contrast the narrower energy spread of the single-nucleon transfer products resulting from the tunneling mechanism.)

If the volume of contact were not excited, nucleons would tend to flow into it, as it would be a region of lower surface energy. This would strengthen the nuclear bond and cause the complete fusion of target and projectile. This is what probably happens at low energy. At higher energies, however, the frictional excitation of the volume of contact should counteract this tendency (in thermodynamic terms, the contact zone has a high vapor pressure). This keeps the bond between projectile

²¹ It should be noted that the maximum in the curve does not necessarily represent the most probable angle of emission. In some collisions the attractive nuclear deflection may exceed the repulsive Coulomb deflection, resulting in emission of the product at a negative angle. This is, of course, experimentally indistinguishable from a deflection to an equal positive angle. The experimental curve (such as Fig. 5) is then a sum of the deflections to a given angle plus deflections past zero degrees to that same angle. This sum need not reach a maximum at the most probable angle of emission. For example, a Gaussian curve centered at 10° with a 20° half-width has ordinates of 10, 8.4, and 5 at 10° , 0° , and -10° , respectively. The sum curve formed by adding ordinates at equal positive and negative angles will then have a peak of 16.8 at 0° and drop to 15 at 10° .

and target weak and allows them to reparate.²² The bond could break at various points resulting in a scattering event, or in the transfer of nucleons.

It is believed that as the bond stretches and breaks, some nucleons and alpha particles may not remain bound to either the projectile or target. This would result in forward peaked distributions of low-energy nucleons and alpha particles, as are believed to have been detected in some preliminary experiments by Knox, Anderson, and Quinton.²³ Such a manner of separation of the grazing nuclei is consistent with the apparently greater tendency of the projectile to lose rather than gain nucleons in a grazing collision (Table II). This bias

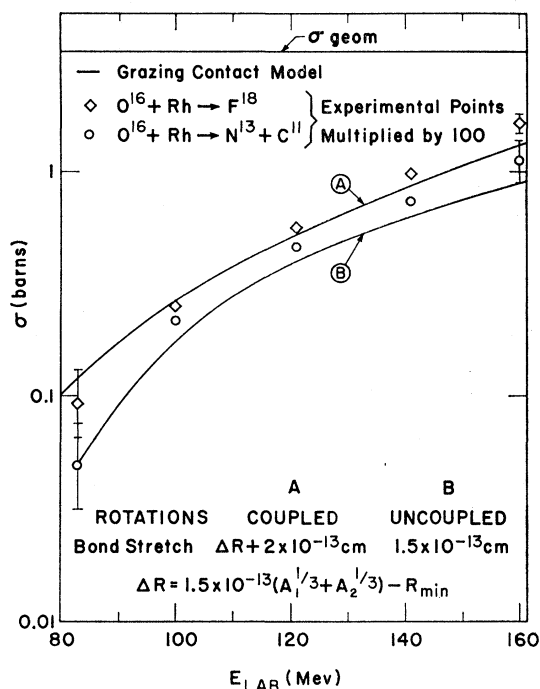


FIG. 14. Shapes of calculated excitation curves compared to experimental data. The excitation energy is taken to equal the kinetic energy of the projectile times the ratio of the volume of overlap to the volume of the projectile. The binding energy between the nuclei is taken to equal 10 Mev per nucleon-nucleon bond. Curve A has been calculated under the additional assumption that the colliding nuclei are rotationally coupled and that the bond between them breaks over a distance $\Delta R + 2 \times 10^{-13}$ cm, where $\Delta R = 1.5 \times 10^{-13} (A_1^{1/3} + A_2^{1/3}) - Z_1 Z_2 e^2 / E$ cm. Curve B results from assuming uncoupled rotation and a bond stretch of 1.5×10^{-13} cm.

²² Separation in a grazing collision could also occur simply because the angular momentum of the system, relative to its mass, is so large that no stable shape of compound nucleus is possible. This would be the case in certain very high-energy collisions, especially between light nuclei. However, for the angular momenta, masses, and energies involved in the systems studied here, equilibrium compound nuclei could exist. For these to be formed, the system must remain bound until the motion of target and projectile become coupled and excitation energy is completely distributed. The reason separation does occur is that, although equilibrium considerations would permit formation of a compound nucleus, the kinetics of the process do not.

²³ W. J. Knox, C. E. Anderson, and A. R. Quinton (private communication).

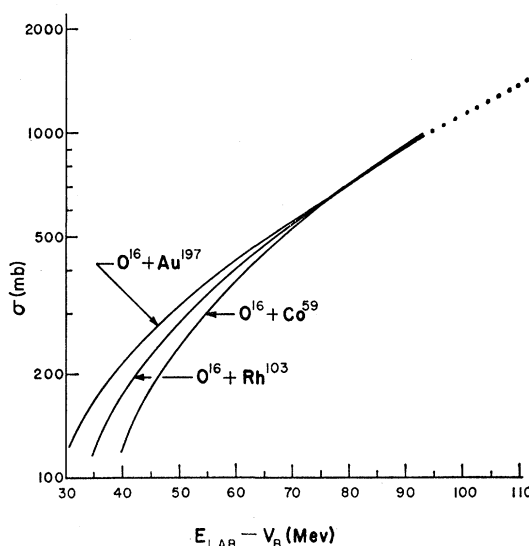


FIG. 15. Calculated cross sections for grazing reactions as a function of the energy above the Coulomb barrier in the laboratory system. Thirty-percent coupling of the rotations is assumed. The binding energy is set equal to one-half of that predicted by the Weizsäcker formula, in approximate agreement with experimental findings. Excitation energy is taken as the kinetic energy of the projectile times the ratio of the volume of overlap to the volume of the projectile plus the binding energy. The radial distance over which the bond breaks is $0.2\Delta R + 0.5f$, where ΔR is defined in Fig. 14. It is expected that multinucleon transfer will not take place if less than one nucleon-nucleon bond is formed, so these curves are cross sections for the formation of one or more nucleon-nucleon bond. The model used will overestimate the cross sections when the volume of overlap becomes an appreciable fraction of the volume of the projectile. These overestimates correspond to the dotted portions of the curves.

toward light products may also be enhanced if some of the products of the grazing reactions are sufficiently excited to subsequently decay by particle emission.

An estimate of the cross section of grazing reactions may readily be made by determining the range of impact parameters satisfying the inequality:

Centrifugal force

$$+ \text{Coulomb force} > \text{nuclear binding force.} \quad (1)$$

This has been done using the methods discussed in Appendix II. The difficulty of estimating the strength of the nuclear bond in the neck and the extent to which it stretches before it gives, makes the results of such a calculation meaningful only as to their orders of magnitude. The two calculated excitation functions in Fig. 14 involve very different assumptions regarding the parameters of the reaction such as excitation energy, degree of coupling, and bond stretching. Both curves show the high threshold and rapid rise of cross section observed for the multinucleon transfer products, but are significantly different from the excitation functions for single-nucleon transfer products formed primarily by barrier processes. However, since the shape of the experimental excitation function can be fitted by a wide range of these parameters, it is not possible to

determine unique values of any of these parameters from the present calculations and experimental results.

Calculated excitation functions for several systems based on the uniform set of assumptions described in the figure caption are shown in Fig. 15. Though the absolute values of these cross sections depend sensitively on the assumptions, the general trends do not. Figures 14 and 15 show that grazing interactions are relatively more important for lighter targets and at higher energies.

The calculations suggest that at high energies (10 Mev per mass unit) the cross section for grazing contact reactions may become a large part of the geometrical cross section. The total cross section of the products detected in the present experiments is about 50 mb. Taking into account unobserved products (e.g., C^{12} , N^{14} , N^{15} , etc.) the total cross section for grazing contact transfer is estimated to be several hundred millibarns. It is also quite plausible that frictional excitation during grazing collisions may cause complete breakup of the projectile, and that this mode of reaction contributes significantly to the total cross section for grazing interactions. The forward distribution of protons and alpha particles with energies of about 10 Mev per mass unit from 160 Mev O^{16} on Ni, which has been observed by Knox, Quinton, and Anderson,²⁰ suggests that the projectile does break up in an appreciable number of cases. This grazing contact mechanism provides a good means of obtaining the very high excitation energies required for such breakup.

Grazing collisions of this nature could well be the mechanism of the "buckshot effect" proposed by Chackett *et al.*¹¹ The buckshot effect postulates that certain products of heavy-ion bombardments could most readily be accounted for by assuming that, in some collisions, only part of the projectile remains bound to the target to form a compound nucleus. Transfer of nucleons to the target is expected to have a high cross section in grazing reactions. A mechanism is thus provided for the formation of a series of compound nuclei having masses relatively near that of the target (or projectile). The calculations of excitation functions of grazing reactions suggest that the buckshot effect should be of relatively greater importance at higher energies and with smaller targets.

A further consequence of the high cross section for grazing reactions, is that the statistical model cannot be applied to the gross results of high-energy heavy-ion reactions. The inadequacy of this model has been pointed out by Hubbard, Main, and Pyle,²⁴ who found that neutron production in heavy-ion bombardment is well below what would be expected from evaporation calculations. To obtain agreement, cross sections for compound nucleus formation significantly less than the interaction cross section (as determined by other means) have to be used, particularly for lighter targets.

²⁴ E. L. Hubbard, R. M. Main, and R. V. Pyle, Phys. Rev. **118**, 507 (1960).

That part of the interaction cross section thus left unaccounted for is of the same order of magnitude as that expected for grazing reactions.

APPENDIX I. EXPERIMENTAL DETAILS

Stacked Foil Experiments

The target assemblies (Fig. 2) for the stacked-foil experiments were mounted in a Faraday cup which measured $1\frac{1}{2}$ inches in diameter by 6 inches long. They were exposed to collimated and analyzed beams of 10^{-9} to 10^{-8} ampere for about 10 minutes. The beam energy was determined to $\pm 2\%$ by a system of deflecting magnets and collimating slits. The Faraday cup was placed in the field of a permanent magnet to prevent loss of charged secondary particles. A second magnet was placed after the last collimating slit to remove low-energy secondary particles and electrons from the beam. Corrections for variations in beam intensity during a run were made by measuring the charge collected in each one or two minute interval and assuming that the beam intensity was constant during each interval.

After irradiation, the target was disassembled and the gold catcher foils placed below end-window beta counters. Identification of product isotopes was based on a good fit to the decay curves. There is little ambiguity in this since only residues of the projectiles could be expected to have sufficient ranges to reach the catchers. The only four such products which have convenient half-lives are F^{18} (112 min), O^{15} (2.1 min), N^{13} (10 min), and C^{11} (20.5 min). No gamma rays were found other than those due to positron annihilation, in agreement with the decay schemes of the expected products.

All decay curves were analyzed graphically, and a few were also analyzed by a least squares fit with a UNIVAC computer. Standard deviations in the least-squares fit and a parameter describing the reliability of the fit were calculated as a part of the computer program. The UNIVAC results showed that the expected half-lives gave a very good fit to experimental decay data. Comparison of results of graphical analysis with results of the least-squares fit gave an indication of errors inherent in the graphical method. Total errors due to decay curve analysis were 10% for products formed in large yields, and as large as 40% for products formed in small yields.

The beta counters were calibrated with a number of standard sources emitting beta particles at various energies. After correction for back scattering and self-absorption, the maximum error in the absolute counting efficiencies is estimated to be 20%. Relative activities are estimated to be accurate to about $\pm 5\%$.

It was determined that changes in the magnetic field near the Faraday cup had relatively little effect on results, indicating that the smallest fields used were capable of preventing appreciable loss of charge from

the Faraday cup by secondary particle emission. Measurements of total cross sections in separate runs, based on the charge collected by the Faraday cup, were reproducible to within 5%. The over-all accuracy of the absolute cross sections are therefore estimated to be from $\pm 20\%$ to $\pm 50\%$ for the various products.

Energies of the products recoiling into the catcher foils were determined from range-energy curves based on a semiempirical plot by Papineau²⁵ of Z_{eff}/Z as a function of $V/Z^{1/3}$, where Z_{eff} is the effective charge of a heavy ion with atomic number Z travelling with velocity V . The range-energy curves were calculated by assuming that over a small energy interval, ΔE , the heavy ions have an average charge given by the graph of Papineau. The distance, Δx , that a heavy ion with this charge will travel in a given material before losing the energy, ΔE , can be determined from experimental range-energy curves of protons in the same target material with the use of the formula:

$$R_z(E/M) = R_p(E/M)M/Z_{\text{eff}}^2. \quad (5)$$

In this expression, $R_z(E/M)$ is the range of an ion with charge Z and energy per mass unit E/M , $R_p(E/M)$ is the range of a proton in the same material with the same energy per mass unit, and M is the ratio of the mass of the ion to the mass of a proton. Ranges determined in this manner were found to agree with experimental values obtained by Northcliff²⁶ to within 5% at the energies of interest.

Angular Distribution Experiments

The apparatus for the measurement of angular distributions is shown in Fig. 4. Before entering the apparatus, the beam was collimated by passing through a $\frac{1}{2}$ -inch diameter iris, and then through a $\frac{1}{4}$ -inch diameter iris at a distance of 22 inches from the first iris. A permanent magnet was placed directly after this collimator to deflect any electrons which might have been emitted through interaction of the beam with the irises. Sixteen inches after the collimator was another $\frac{1}{2}$ -inch diameter iris to remove particles which had been scattered by the collimator. The beam then entered the target chamber, which was electrically insulated from the rest of the apparatus and served as the Faraday cup. The target chamber was a cylinder 4 inches in diameter and 20 inches long, and was machined so that the target holder and catcher foil holders would slide inside. The target holder was a hollow cylinder about 6 inches in length having a $\frac{3}{4}$ -inch diameter hole at either end, with the target mounted immediately beyond the second $\frac{3}{4}$ -inch hole. The products of interest recoiled from the target and were stopped in copper catcher foils taped to the inside of the catcher foil holders and to the end plate. Each catcher stopped products emitted from the target in a certain angular interval. All catcher foils

were covered by a thin (3–6 mg/cm²) screening foil to stop short range heavy target residues which recoil from the target.

Full energy (10 Mev per mass unit) beams of C¹², N¹⁴, O¹⁶, and F¹⁹, and beams of O¹⁶ with energies down to 80 Mev were used to irradiate a 7.35-mg/cm² Rh target. Beam intensities were usually 5×10^{-9} to 50×10^{-9} ampere.

After irradiation, the catcher foils were removed from the target chamber and placed in scintillation counters. The outputs were fed into single-channel analyzers which were adjusted to accept the positron annihilation gamma-ray pulses. Products were again identified by decay-curve analysis. The same four products that were observed in the stacked foil experiments were found.

A correction was made for activity produced by the portion of the beam which was scattered in the target and which then reacted on striking the catcher foils. To illustrate the correction, assume only one product of interest was formed in the target, and that an O¹⁶ beam was used. Consider two catcher foils [Fig. 16(a)], one at zero degrees to the beam direction (catcher 1) and one at some other angle (catcher 2). The total cross section for all multinucleon transfer products of interest in a typical experiment is about 50 mb, and this was distributed over a number of catcher foils. The total cross section for all products formed by beam particles striking the catcher is of the order of barns. Therefore, the activity that was produced in the target and which then recoiled into catcher 1 is negligible compared to the activity produced by the O¹⁶ beam as

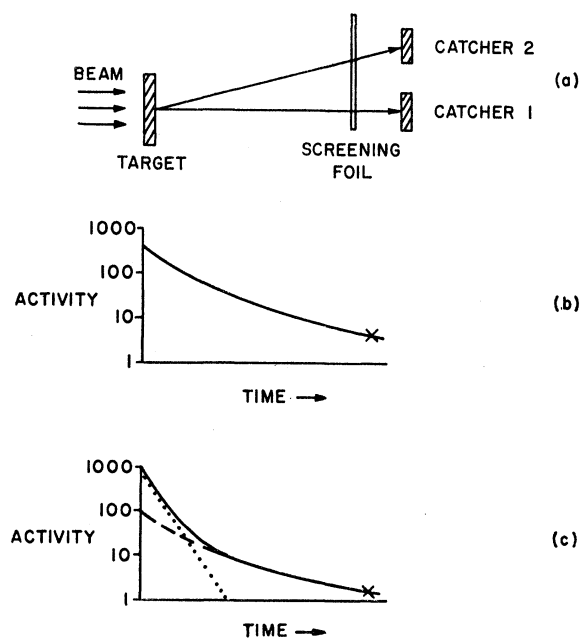


FIG. 16. Illustration of the corrections for activity produced by beam particles which are scattered in the target and then react upon striking the catcher foils.

²⁵ M. A. Papineau, *Comp. rend.* **242**, 933 (1956).

²⁶ L. C. Northcliff (private communication).

it was stopped in catcher 1. It is therefore assumed that the decay curve of catcher 1 [Fig. 16(b)] represents decay of products which are formed by O^{16} striking any catcher foil.

The decay curve of catcher 2 represents products originating at two sources. Some products were formed as scattered O^{16} reacted with the catcher foil, and some products were formed in the target and recoiled into the catcher. The observed decay curve for catcher 2 is shown as the solid curve of Fig. 16(c). This decay was followed until activity due to expected transfer products originating in the target was negligible [the point marked \times in Fig. 16(c)]. A curve parallel (on a logarithmic activity scale) to the decay curve for catcher 1 was drawn through this point [dashed curve in Fig. 16(c)] and then subtracted from the observed decay curve. This gave the activity which was formed in the target and recoiled into catcher 2 [dotted curve in Fig. 16(c)]. Results were discarded if activity due to scattered O^{16} was greater than the activity of the transfer products. This had to be done at the smallest angles; however, at larger angles the scattering correction was small.

Transformations from laboratory angles to center-of-mass angles were made according to Marion *et al.*²⁷—assuming that all products were formed in their ground states. This transformation is not very sensitive to energy changes, so errors due to formation of products in excited states are not serious. All angles in this paper are given in the center-of-mass system.

The determination of the total charge collected should be accurate to about $\pm 5\%$. This error is smaller than in the stacked-foil experiments because loss of secondary particles is more severely limited by geometry. Counting efficiencies were known to about $\pm 5\%$ due to the use of gamma-ray counting techniques. Each of the ten counters was calibrated before and after each run by a standard Na^{22} source, and the variation of efficiency was seldom greater than 2% of the efficiency. Samples were placed in small aluminum containers during counting in order to insure annihilation of positrons in a definite volume, and corrections were made for absorption of gamma rays in the container and in the sample itself. A positron branching ratio of 90% was assumed²⁸ and background due to the 1.28-Mev gamma ray was subtracted. The main source of error at small angles was due to the subtraction of activity produced by the scattered beam discussed above. The upper limit of this error was arbitrarily set as being equal to 50% of the correction itself. The magnitude of this error is indicated on Fig. 5.

An additional 10% error is introduced in the integrated thin-target cross sections (Table II) by the necessity of having to extrapolate the curves (Fig. 5) to zero degrees. The cross sections quoted in Table II

are therefore accurate to $\pm 20\%$ for values greater than 10 mb and are as poor as $\pm 50\%$ for some values near 1 mb.

APPENDIX II. CALCULATIONS BASED ON THE GRAZING CONTACT MODEL

The calculations used to obtain excitation functions for grazing reactions (Figs. 14 and 15) are outlined in this section. The calculations are based on rather crude classical assumptions, but are useful for prediction of qualitative trends and cross sections to within an order of magnitude. The actual calculations are available in the thesis of one of the authors²⁹; and in this discussion only the method and assumptions of the treatment are presented. The cross section for grazing collisions is computed by estimating the range of impact parameters for which

(1) the closest approach of centers is less than the sum of the radii of the undistorted nuclei, and (2) Coulombic and centrifugal forces at the distance of closest approach exceed nuclear binding forces, so that the system separates.

The main part of the calculation is an approximation of the forces between the projectile and target at the distance of closest approach. At this point, the system is assumed to have the form of overlapping spheres; i.e., no nucleons have flowed into or out of the region of contact. It is further assumed that the kinetic energy of the nucleons in the projectile which actually come into contact with the target is converted into excitation energy, but that the nucleons outside the volume of overlap or contact retain their collective kinetic energy. This assumption essentially states that, outside the volume of contact, the target and projectile remain rotationally uncoupled. As discussed in the text, this assumption, though probably substantially correct, cannot be wholly so. Because of this, a calculation making the opposite assumption, complete coupling, was also made and will be mentioned later.

The binding energy of the system is computed by calculating the reduction in surface energy of the nuclei in contact. The magnitude of this surface energy is taken from the Weizsäcker equation³⁰ and comes to about 10 Mev per nucleon-nucleon bond. The actual binding energy is almost certainly less than this because of the excitation of the area of contact. The resulting overestimate of the binding force will tend to make the calculated grazing cross sections too small.

An estimate of the binding energy required to account for the experimental angular distribution was made as follows. The assumptions are that a uniform attractive force acts perpendicular to the trajectory of the projectile during the time of interaction. It is estimated from geometry that the projectile travels tangentially around

²⁷ J. B. Marion, T. I. Arnette, and H. C. Owens, Oak Ridge National Laboratory Report ORNL-2574, 1959 (unpublished).

²⁸ R. Sherr and R. M. Miller, *Phys. Rev.* **93**, 1076 (1954).

²⁹ Richard Kaufmann, thesis, Yale University, New Haven, Connecticut, 1960 (unpublished).

³⁰ C. F. von Weizsäcker, *Z. Physik* **96**, 431 (1935).

the target for a distance of 5–10 f, and the radial distance over which interaction is appreciable is 1–3 f. With these assumptions, the binding energy required to deflect the observed products from the Rutherford scattering cutoff of 24° to an angle of 10° is about 10 Mev.

The forces at the moment of closest approach can now be calculated for a given bombarding energy and distance of closest approach using the equations for the conservation of energy and angular momentum. The Coulomb repulsive force is calculated for point charges. The rotational force is computed from the kinetic energy at the moment of closest approach. This energy is equal to the bombarding energy minus the Coulomb and the excitation energies. In the uncoupled model, the excitation energy is just the kinetic energy of the nucleons in the projectile which come into contact with the target plus the binding energy. The average attractive force between the nuclei can be calculated by assuming the binding energy decreases uniformly as the bond stretches and the system separates. This force is just the total binding energy divided by the distance over which the bond breaks. Various estimates of this distance were used to calculate the curves in Figs. 13 and 14. All estimates were of the form $a\Delta R + b$, where ΔR is the radial distance of overlap and a and b are parameters; i.e., all bonds stretch to some extent, but the stretching will increase as the overlap increases. Only the ratio of the binding energy to the distance of stretching appears in the calculations.

Numerical calculations for an O^{16} beam on a Rh target show that repulsive forces are greater than attractive forces at the moment of closest approach for interactions in which as many as four nucleon-nucleon bonds are formed. This conclusion holds for all reasonable values of the parameters. If the bond does not break uniformly, but does so over a small distance, the attractive force would be increased. However, in order to overcome the repulsive forces at the highest energies available, unreasonable assumptions concerning bond stretching must be made. For example, a 40-Mev bond must break over a distance of 0.4 f or less to overcome repulsive forces at the highest bombarding energy.

This model would be expected to break down when the region of contact approaches an appreciable fraction of the projectile volume. Then it would no longer be valid to consider a two-body system with a weak bond in the region of contact. For this reason, a four nucleon-nucleon pair bond, which corresponds to an overlap of 2–3 f (diameter of O^{16} is 7–8 f), is about the maximum bonding that should be considered.

The range of impact parameters, and hence the cross section for which contact is made but for which the repulsive Coulombic and centrifugal forces exceed the nuclear binding forces, can now be calculated. The result of such a calculation for O^{16} plus Rh^{103} is given in curve *B* of Fig. 14. Curve *A* results from a similar treatment in which the colliding nuclei have become rotationally coupled. To reduce their relative velocity at the point of contact to zero, the frictional energy loss and the resulting internal excitation are much larger for the coupled than for the uncoupled model. As discussed in the text, the uncoupled system is probably a much better representation of the actual interaction. Nevertheless, it is interesting that on either model a substantial cross section for grazing reactions may be expected. This is perhaps the most important conclusion of these calculations: that though a number of important assumptions are made, the qualitative result that grazing reactions should occur does not appear sensitively dependent on the validity of these assumptions.

ACKNOWLEDGMENTS

The authors are most grateful to J. McIntyre, both for permitting our use of his counting equipment and for his interest and helpfulness. Discussions of this work with G. Breit were most stimulating and are greatly appreciated. We are deeply indebted to H. Mullish, who supplied and supervised the running of the UNIVAC program.

The very considerable help and, at times, the patience and forbearance of the heavy-ion accelerator staff is gratefully acknowledged.